Conformations of Unsolvated Glycine-Based Peptides

Robert R. Hudgins[†] and Martin F. Jarrold*

Department of Chemistry, Northwestern University, 2145 Sheridan Road, Evanston, Illinois 60208

Received: October 6, 1999; In Final Form: January 6, 2000

The conformations of unsolvated glycine-based peptides have been probed using high-resolution ion mobility measurements and molecular dynamics simulations. Alanine-based Ac-Ala$_n$-LysH$^+$ peptides have previously been shown to form helices in the gas phase. In contrast, the polyglycine analogues (Ac-Gly$_n$-LysH$^+$) do not form helices at room temperature; they adopt random globular conformations. Thus, the stabilities of alanine and glycine helices in vacuo are consistent with the helix propensities in aqueous solution, where alanine has the highest helix propensity and glycine has one of the lowest.

Introduction

The helix propensities of the different amino acids in solution[1−4] are influenced to some extent by the solvent.[5−7] Solvent effects can be probed by examining helix formation in vacuo.[8−11] Such studies should ultimately provide a thermodynamic scale of intrinsic helix propensities, which could then be used to quantitatively measure the effects of the solvent. We recently reported studies of the conformations of protonated polyglycine, Gly$_n$H$^+$, and polyalanine, Ala$_n$H$^+$, peptides in the gas phase.[9] These peptides were selected because of their dramatically different helix propensities in aqueous solution; alanine has the highest helix propensity while glycine has one of the lowest.[1−4] However, our studies showed that for $n \leq 20$, both oligomers adopt random globular conformations. The failure to form helical states in vacuo appears to be at least partly related to the charge. It is the N-terminus that is protonated in these peptides, and since the N-terminus is at the positive end of the helix macrodipole,[12] protonating it destabilizes the helical conformation.

We have recently shown that a stable polyalanine helix can be generated in vacuo by adding a lysine at the C-terminus.[10,11] In Ac-Ala$_n$-LysH$^+$ peptides it is the lysine side-chain that is protonated. The helical conformation is stabilized by interaction of the charge with the helix dipole and by helix-capping: hydrogen bond formation between the protonated lysine side chain and the dangling carbonyl groups at the C-terminus of the helix.[13−15] If the lysine is moved to the N-terminus, the helical conformation is destabilized and Ac-LysH$^+$-Ala$_n$ peptides adopt globular conformations. Since we now know how to stabilize alanine helices in the gas phase, it is appropriate to reexamine the difference between alanine and glycine peptides to determine whether the solution phase helix propensities are reflected in the gas phase.

In this manuscript we report molecular dynamics (MD) simulations and experimental studies of the conformations of the glycine analogues of the alanine peptides described above. We anticipate that polyglycine peptides with a lysine at the N-terminus, Ac-LysH$^+$-Gly$_n$ will not form a helix, like its alanine analogue. However, for Ac-Gly$_n$-LysH$^+$ peptides the helical conformation should be stabilized by the same features that stabilize the Ac-Ala$_n$-LysH$^+$ helices: helix capping and the interaction of the positive charge with the helix dipole. So whether the Ac-Gly$_n$-LysH$^+$ peptides form helices provides a simple way to test the relative stabilities of the helical conformation for unsolvated glycine and alanine oligomers.

Molecular Dynamics Simulations

Molecular dynamics (MD) simulations were performed using the MACSIMUS Molecular Modeling Software[16] with CHARMM-like potentials (21.3 parameter set).[17] The bond lengths were constrained by SHAKE,[18] and CH, CH$_2$, and CH$_3$ units were treated as united atoms.[19] In both the Ac-Lys-Gly$_n$ and Ac-Gly$_n$-Lys peptides the protonation site is assumed to be the nitrogen in the lysine side chain (protonation at the N terminus is blocked by acetylation). The lysine side chain has the highest pK_a in solution, and gas-phase basicity measurements for individual amino acids and small peptides are consistent with protonation at the side chain amine.[20−22] The simulations were performed with a time step of 1 fs. A dielectric constant of 1, which is appropriate for small peptides in a vacuum, was used. Multiple simulations of 0.25−1.0 ns were performed for each peptide at 300 K. The starting structures employed were usually either an ideal α-helix or a fully extended, all-trans geometry. Other starting geometries were used in a few cases (see below). The extended geometries rapidly collapsed to random globular conformations in the simulations. Three simulations were typically performed for each peptide starting from the extended conformation with different initial conditions. An average energy was determined from the last 60 ps of each MD run. The average energies of the three MD runs typically performed for each peptide usually differed by ∼20 kJ mol^{-1}. The results from the lowest energy simulation were used for further analysis. Single MD simulations were performed for each peptide starting from the helical conformation. Average energies were again determined from the last 60 ps. Some simulations were also performed at elevated temperatures to observe large-scale conformational changes on the MD time scale. These are discussed in more detail below.

The most energetically stable structures found in MD simulations for the Ac-Gly$_n$-LysH$^+$ peptides were helical. An example of an Ac-Gly$_{19}$-LysH$^+$ helix is shown in Figure 1a. This structure was generated from an α-helix, but during the simulation it relaxed to a partial π-helix. A π-helix has *i*,*i*+5

[†] Present address: Institute for Physical Chemistry, University of Basel, Klingelbergstrasse 80, CH-4056 Basel, Switzerland.

10.1021/jp9935539 CCC: $19.00
Published on Web 02/10/2000

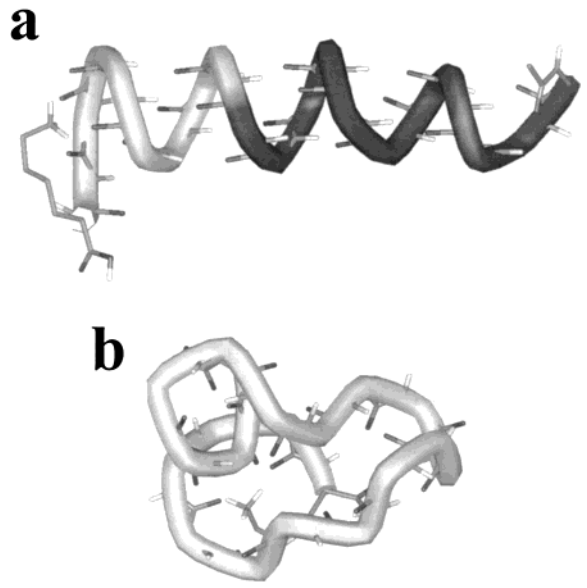

Figure 1. Structures generated in the MD simulations for the Ac-Gly_{19}-$LysH^+$ peptide. (a) shows a partial α- and partial π-helix, and (b) shows a globular conformation.

hydrogen bonds (4.4 residues per turn) instead of the $i,i+4$ hydrogen bonds (3.6 residues per turn) in an α-helix. Simulations started from α-helices, 3_{10}-helices ($i,i+3$ hydrogen bonds, 3 residues per turn), and π-helices, all quickly rearranged to partial α- and partial π-helices like that shown in Figure 1a. Left-handed Ac-Gly_n-$LysH^+$ helices were found to be slightly less stable (∼15 kJ mol^{-1}) than right-handed ones, presumably because of differences due to the L-lysine at the C-terminus. MD simulations performed for uncharged Gly_n helices suggest that the α-helix is more energetically stable than the π-helix for neutral peptides. However, in MD simulations using the GROMOS force field, DiCapua and collaborators found that uncharged polyglycine α-helices rearranged into π-helices.[7] So the relative energies of the α- and π-helices in the uncharged peptide are sensitive to the details of the force field. To test this sensitivity for Ac-Gly_n-$LysH^+$ peptides, some calculations were performed with AMBER. The AMBER calculations were performed on HyperChem 5.02 (Hypercube Inc., Gainesville, FL) using the AMBER3 parameter set. The all-atom potential and the united atom approximation[19] were used for separate simulations at 300 K. AMBER reproduced the partial π-/partial α-helix found for Ac-Gly_n-$LysH^+$ with CHARMM. So with the CHARMM and AMBER potentials used in this work it seems that the partial π-helix in the Ac-Gly_n-$LysH^+$ peptides is induced by the charge at the C-terminus: because of the extra residue per turn, the π-helix has an additional carbonyl group available to hydrogen bond to the protonated amine of the lysine (see Figure 1). The α-helix persists at the N-terminus of these peptides presumably because it has one fewer dangling N−H group than the π-helix.

A competing, though less energetically stable structure is a "self-solvated" random globule, shown for Ac-Gly_{19}-$LysH^+$ in Figure 1b. The globules were generated by starting the simulations from fully extended, all-trans conformations. In the globules, the backbone carbonyls of the peptide "solvate" the charge, and the rest of the peptide wraps around to maximize these interactions. The globular structure was found to be ∼70 kJ mol^{-1} less stable than the helical one for Ac-Gly_{19}-$LysH^+$. However, at 300 K the globules were not observed to convert into helices (and the helices did not convert into globules) on the nanosecond time scale of the simulations. Two simulations were performed at 700 K for Ac-Gly_{19}-$LysH^+$ starting from an α-helix. In both simulations the helix completely melted and then the conformation fluctuated rapidly. In one simulation the helix melted within 60 ps, while in the other a short helical fragment persisted out to around 200 ps before it also completely disappeared.

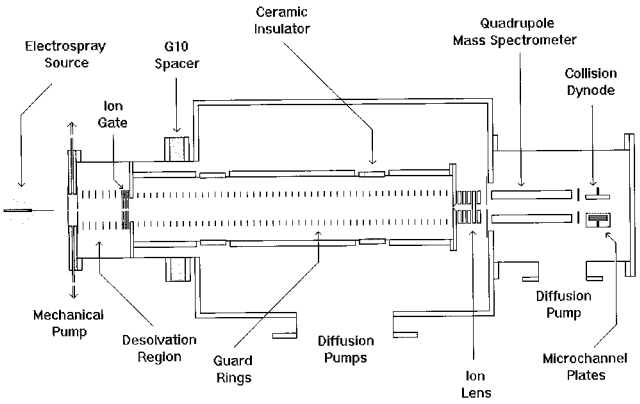

Figure 2. Schematic diagram of the high-resolution ion mobility apparatus.

If the lysine is moved from the C-terminus to the N-terminus of the glycine polypeptides the hydrogen bonding and charge−dipole stabilization of the helical state vanish, and random globular conformations are expected to be more stable than helical ones. MD simulations at 300 K for Ac-$LysH^+$-Gly_n peptides that were started as α-helices rapidly collapsed to globular states. The Ac-$LysH^+$-Gly_n globules have similar energies to the Ac-Gly_n-$LysH^+$ globules.

Experimental Methods

High-resolution ion mobility measurements[23,24] were performed for a range of Ac-Gly_n-$LysH^+$ and Ac-$LysH^+$-Gly_n peptides to examine their conformations. The mobility is a measure of how rapidly an ion moves through an inert buffer gas under the influence of a weak electric field.[25] The mobility depends on the ion's collision cross section with the buffer gas, and the cross section depends on the conformation.[26] Our experimental apparatus, shown schematically in Figure 2, consists of an electrospray source, a 63 cm long drift tube containing helium buffer gas, and a quadrupole mass spectrometer. The ions are electrosprayed in air and enter the apparatus through a 0.125 mm aperture. They initially enter a small differentially pumped region where a substantial fraction of the air and solvent that comes in with the ions through the entrance aperture is pumped away, along with helium buffer gas that enters from the other side. The ions are drawn through this volume by an electric field and then enter a desolvation region maintained at room temperature. After passing through the desolvation region, the ions pass through the ion gate and enter the drift tube. The ion gate consists of a cylindrical channel, 0.5 cm in diameter and 2.5 cm long. A helium buffer gas flow of 900−1800 sccm prevents solvent and air molecules from entering the drift tube from the desolvation region, while an electric field of 400 V/cm carries the ions through against the buffer gas flow. The drift tube has 46 drift guard rings, coupled to a voltage divider, to provide a uniform electric field along its length. A drift field of 160 V cm^{-1} was employed along with a helium buffer gas pressure of around 500 Torr. After traveling along the length of the drift tube, some of the ions exit through a 0.125 mm diameter aperture and are focused into a quadrupole mass spectrometer. Following mass analysis, the ions are detected by an off-axis collision dynode and dual

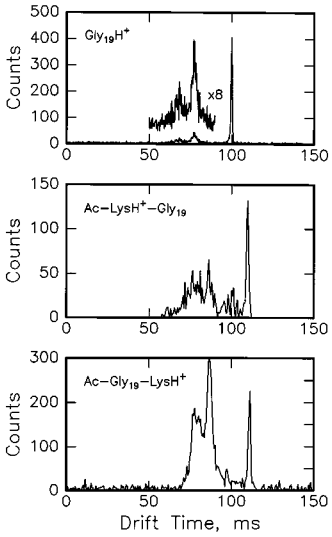

Figure 3. Drift time distributions measured for $Gly_{19}H^+$, Ac-$LysH^+$-Gly_{19}, and Ac-Gly_{19}-$LysH^+$. The distributions have been normalized to a temperature of 298 K and a helium buffer gas pressure of 525 Torr.

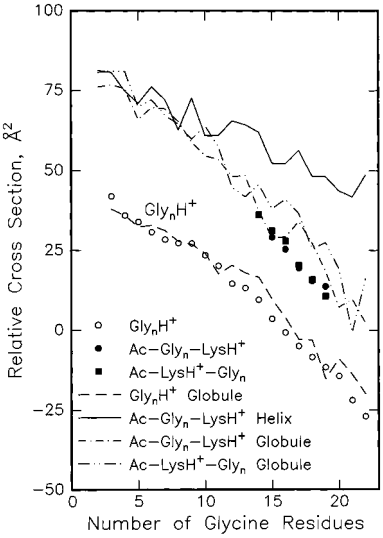

Figure 4. Plot of the measured and calculated relative collision cross sections against the number of glycine residues for Gly_nH^+ (○), Ac-Gly_n-$LysH^+$ (●), and Ac-$LysH^+$-Gly_n (■) peptides. The dashed lines show relative collision cross sections calculated for Gly_nH^+. The dashed−dotted lines show cross sections calculated for the Ac-Gly_n-$LysH^+$ and Ac-$LysH^+$-Gly_n globules. The solid line shows cross sections calculated for Ac-Gly_n-$LysH^+$ helices.

microchannel plates. Drift time distributions are recorded by switching the voltages on a pair of half plates in the ion gate so that a short packet of ions (usually around 750 μs) is admitted to the drift tube. The arrival time distribution of the packet of ions is recorded at the detector with a multichannel scaler. Ac-Gly_{19}-Lys and Ac-Lys-Gly_{19} peptides were synthesized by Anaspec (Anaspec Inc., San Jose, CA) and used without purification. In each case there is a distribution of peptide sizes present because of inefficient coupling in the Fmoc synthesis. The presence of a distribution of sizes is not a concern in our measurements, because specific peptides can be mass selected. The peptides were electrosprayed in formic acid.

Experimental Results

Figure 3 shows drift time distributions measured for $Gly_{19}H^+$, Ac-$LysH^+$-Gly_{19}, and Ac-Gly_{19}-$LysH^+$. The drift time distribution for $Gly_{19}H^+$ was taken from our previous work on polyglycine peptides.[9] For this peptide the distribution consists of a dominant, sharp peak at around 100 ms and broad, low-intensity features between 60 and 90 ms. The sharp peak at around 100 ms is due to the $Gly_{19}H^+$ monomer, while the broad features between 60 and 90 ms are due to dimers and other multimers with the same m/z ratio as $Gly_{19}H^+$.[27] This is confirmed by performing drift time measurements at m/z ratios that do not correspond to monomers. For example, the mixed dimer $(Gly_{18}H{\cdot}Gly_{19}H)^{2+}$ has a m/z ratio halfway between $Gly_{18}H^+$ and $Gly_{19}H^+$. Drift time distributions measured at m/z ratios corresponding to the mixed dimers have the broad features at shorter drift times but lack the sharp peak at longer drift time assigned to the monomer. Drift time distributions measured for the Ac-$LysH^+$-Gly_n and Ac-Gly_n-$LysH^+$ peptides show the same general features as the Gly_nH^+ distributions: a sharp peak at long drift times due to the monomer and a broad distribution at shorter times due to dimers and other multimers (see Figure 3). In the distributions shown for Ac-$LysH^+$-Gly_{19} and Ac-Gly_{19}-$LysH^+$ in Figure 3 the dimer and multimer peaks are larger than for $Gly_{19}H^+$. For Ac-Gly_{19}-$LysH^+$ the dimer peak is even larger than the monomer peak at around 110 ms. The amount of dimer and other multimers present in these drift time distributions appears to be a strong function of the electrospray and solution conditions. We have recorded drift time distributions for glycine peptides under different conditions that show a much higher multimer abundance than is apparent in Figure 3 for $Gly_{19}H^+$. So the larger dimer and multimer abundance for Ac-Gly_{19}-$LysH^+$ in Figure 3 does not necessarily indicate that Ac-Gly_n-$LysH^+$ dimers and multimers are more thermodynamically stable than the dimers and multimers of the other peptides.

The measured drift times, t_D, of the monomers, obtained from the drift time distributions, are converted into average collision cross sections using[25]

$$\Omega_{avg}^{(1,1)} = \frac{(18\pi)^{1/2}}{16}\left[\frac{1}{m}+\frac{1}{m_b}\right]^{1/2}\frac{ze}{(k_BT)^{1/2}}\frac{t_DE}{L}\frac{1}{\rho} \qquad (1)$$

In this expression, m is the mass of the ion, m_b is the mass of a buffer gas atom, ze is the charge on the ion, ρ is the buffer gas number density, L is the length of the drift tube, and E is the drift field. Independent measurements of the cross sections almost always agree to within 1% (<2.5 Å^2). Relative collision cross sections derived from the mobility measurements for Ac-Gly_n-$LysH^+$, $n = 15-19$, Ac-$LysH^+$-Gly_n, $n = 14-19$, and Gly_nH^+, $n = 3-22$, are plotted against n in Figure 4. The relative cross section scale employed here is defined by $\Omega_{avg}^{(1,1)} - 11.86n$ where the cross section, $\Omega_{avg}^{(1,1)}$, is in Å^2 and 11.86 Å^2 is the average cross section per residue determined for an ideal polyglycine α-helix with torsion angles fixed at $\phi = -57°$ and $\psi = -47°$. With this scale, α-helices have relative cross sections that are independent of the number of glycine residues, and other conformations have relative cross sections that change with n. For example, using the analogous scale for alanine, relative cross sections for the Ac-Ala_n-$LysH^+$ peptides are independent of n for $n \geq 7$, indicating that they have α-helical conformations. The lines in Figure 4 show average cross sections derived from the MD simulations. These were evaluated by averaging the cross sections for 50 structures saved at regular intervals throughout the simulations. The cross sections for the individual structures were determined by the trajectory method of Mesleh et al.[28] For species with well-defined rigid geometries we have

come to expect the calculated mobility to be within 2% of the measured quantity (if the correct structure is used for the mobility calculations).[29] The lines show significant fluctuations on going from one peptide to the next**;** these fluctuations result from incomplete conformational averaging during the limited time scale of the MD simulations.

The solid line in Figure 4 shows relative cross sections determined for the Ac-Gly_n-$LysH^+$ helices from the MD simulations. As noted above, α-helices will give relative cross sections that are independent of *n*. The decreasing relative cross sections for the Ac-Gly_n-$LysH^+$ helices result because they are partial α- and partial π-helices. The dashed−dotted lines show relative cross sections calculated for the globular conformations. They decrease significantly with increasing *n* because these conformations are substantially more compact than α-helices. The open points in Figure 4 are measured relative cross sections for protonated polyglycine peptides, Gly_nH^+, taken from ref 9. The measured cross sections are in good agreement with the cross sections determined for globular conformations of these peptides (dashed line).

The measured relative cross sections for the Ac-$LysH^+$-Gly_n peptides (solid squares) in Figure 4 are close to the calculated cross sections for the Ac-$LysH^+$-Gly_n globules (dashed−dotted line). With the lysine at the N-terminus, hydrogen bonding and charge−dipole stabilization of the helical state vanish, and thus globular conformations are expected for the Ac-$LysH^+$-Gly_n peptides. However, the measured relative cross sections for the Ac-Gly_n-$LysH^+$ peptides (solid circles), which are predicted to be helical, are not in good agreement with the cross sections calculated for the helical conformations of these peptides. In fact, the measured cross sections for the Ac-Gly_n-$LysH^+$ peptides are very close to those measured for the Ac-$LysH^+$-Gly_n peptides. These results indicate that the Ac-Gly_n-$LysH^+$ peptides adopt random globular conformations. While the measured cross sections for the Ac-Gly_n-$LysH^+$ and Ac-$LysH^+$-Gly_n peptides are close to the calculated cross sections for the globules, the measured cross sections are often slightly smaller than the calculated ones. The calculated cross sections for the Ac-Gly_n-$LysH^+$ and Ac-$LysH^+$-Gly_n globules shown in Figure 4 are average cross sections for the lowest energy globules obtained by starting the simulations from fully extended, all-trans conformations. In many cases the calculated cross sections differ from the measured ones by significantly more than the 2% error margin usually found with rigid geometries.[29] The fluctuations in the calculated cross sections suggest that the problem is mainly due to inadequate conformational averaging. A better sampling scheme may identify slightly lower energy structures for many of the peptides, and better averaging should lead to improved agreement between the measured and calculated cross sections.

Discussion

The MD simulations for both Ac-Gly_n-$LysH^+$ and Ac-Ala_n-$LysH^+$ peptides indicate that a helix is the lowest energy conformation. However, the helix is not observed for the Ac-Gly_n-$LysH^+$ peptides at room temperature. Figure 5 shows a plot of the energy difference, from the MD simulations, between the globular and helical states of the Ac-Gly_n-$LysH^+$ and Ac-Ala_n-$LysH^+$ peptides. There are an enormous number of globular conformations, and because of the limited time scale of the MD simulations it is not possible to sample all of them. Previous studies of protonated polyglycine and polyalanine indicate that these peptides do not have a single well-defined globular conformation at room temperature, they have structures that

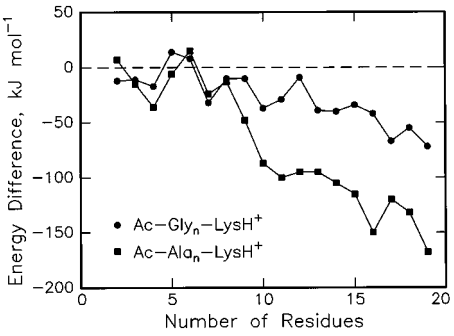

Figure 5. Plot of the energy difference (from MD simulations) between the helical and globular conformations of the Ac-Gly_n-$LysH^+$ and Ac-Ala_n-$LysH^+$ peptides.

change rapidly on the time scale of the measurements.[9] The fluctuations in the energy differences between the helical and globular conformations apparent in Figure 5 result from incomplete conformational averaging. However, it is clear that the energy difference for the glycine peptide is substantially smaller than the corresponding difference for the alanine analogues (∼170 kJ mol^{-1} for Ac-Ala_{19}-$LysH^+$ versus ∼70 kJ mol^{-1} for Ac-Gly_{19}-$LysH^+$). The difference in these relative stabilities is primarily due to differences in the stabilities of the globules and appears to result mainly from a significantly more negative electrostatic energy in the Ac-Gly_n-$LysH^+$ globules and a less unfavorable strain energy. This suggests that the Ac-Gly_n-$LysH^+$ globules are more energetically favorable than their alanine analogues because they are able to twist upon themselves to form a greater number of well-aligned hydrogen bonds, while incurring less strain energy. To determine whether the relative energies of the helical and globular conformations of the Ac-Gly_n-$LysH^+$ and Ac-Ala_n-$LysH^+$ peptides were sensitive to the force field employed, some calculations were performed with AMBER using both the all-atom potential and the united atom approximation.[19] The relative energies of the different conformations were similar to those found with the CHARMM-like potentials. As described above, the Ac-Gly_{19}-$LysH^+$ helix rapidly melts in simulations performed at 700 K. In contrast, in a 1 ns 700 K simulation for Ac-Ala_{19}-$LysH^+$, the helix persisted, albeit with a considerable amount of fraying particularly from the N-terminus. At one point in the simulation over half of the helix had unraveled, but it refolded again. It is also interesting to note that at the elevated temperature a π-helix often propagated from the C-terminus of the Ac-Ala_{19}-$LysH^+$ peptide and then receded back again to give a pure α-helix. Partial π-helices were not observed in the 300 K simulations of the alanine-based peptides.

While the MD simulations clearly indicate that the helical conformations of the Ac-Gly_n-$LysH^+$ peptides are energetically favored over the globule, it is the free energy that determines the favored conformation at room temperature. Recent estimates from multicanonical Monte Carlo simulations suggest that the $-T\Delta S$ term for the helix to coil (or globule) transition in a vacuum is around −115 kJ mol^{-1} for Ala_{20} at 300 K.[26] The energy difference between the Ac-Ala_{19}-$LysH^+$ helix and globule is around 170 kJ mol^{-1} according to MD simulations. This energy difference approximately equals ΔH so the free energy (ΔG) still favors the helix for Ac-Ala_{19}-$LysH^+$ at room temperature (see Table 1). For Ac-Gly_{19}-$LysH^+$, however, the energy difference between the helix and globule in the simulations (ΔH) is substantially less, only around 70 kJ mol^{-1}. In addition, the entropy difference is expected to be larger for glycine than for alanine because of the greater conformational

TABLE 1: Comparison of Estimated ΔH, $-T\Delta S$, and ΔG for the Helix to Random Globule Transition in Ac-Ala$_{19}$-LysH$^+$ and Ac-Gly$_{19}$-LysH$^+$ Peptides

peptide	ΔH,[a] kJ mol^{-1}	$-T\Delta S$,[b] kJ mol^{-1}	ΔG, kJ mol^{-1}
Ac-Ala$_{19}$-LysH$^+$	170	−115	+55
Ac-Gly$_{19}$-LysH$^+$	70	−170	−100

[a] From energy difference in MD simulations. [b] From multicanonical Monte Carlo simulations in ref 30 and from ref 31.

freedom of glycine. This is estimated to contribute at least another 50−60 kJ mol^{-1} to the $-T\Delta S$ term[31] for Ac-Gly$_{19}$-LysH$^+$. So the $-T\Delta S$ term for helix to globule transition of the glycine peptide is expected to be around −170 kJ mol^{-1}, and at room temperature the free energy favors the globular conformation (see Table 1). This is consistent with the experimental observations. MD simulations incorporate entropy implicitly, and an MD trajectory should spend most of its time in the lowest free energy structure (which is not necessarily the structure with the lowest energy or enthalpy). However, this is only true if the trajectory is run long enough. The reason that the energetically favored Ac-Gly$_n$-LysH$^+$ helices do not collapse into the lower free energy globules in the simulations is that nanosecond trajectories are not long enough to explore the necessary phase space.

From the results presented here it appears that the stabilities of alanine and glycine helices in vacuo are consistent with the helix propensities in solution. This supports the view that the solution helix propensities are determined mainly by intramolecular forces.[1,32,33] Differences in the stabilities of glycine and alanine helices have been found in previous in vacuo simulations.[30,34−36] In recent MD simulations in an implicit solvent, neutral Gly$_{20}$ peptides were found to form an α-helix much less frequently than Ala$_{20}$ peptides,[37] even though the helix was found to be the energetically favored state for both Gly$_{20}$ and Ala$_{20}$. In solution, the low helix propensity of glycine is usually attributed to its large conformational freedom, which makes the nonhelical state favored entropically.[1,31] In vacuo, both entropy and energy appear to contribute to the low helix propensity. If the temperature is lowered, however, the $T\Delta S$ term will become smaller and ultimately the free energy should favor the helical conformation for the Ac-Gly$_n$-LysH$^+$ peptides. Conversely, raising the temperature should melt the Ac-Ala$_n$-LysH$^+$ helices. Experiments to determine the transition temperatures are currently in progress.

Acknowledgment. We thank Jiri Kolafa for the use of his MACSIMUS Molecular Modeling Software. We gratefully acknowledge the National Science Foundation, The National Institutes of Health, and the donors of the Petroleum Research Fund, administered by the American Chemical Society, for partial support of this work.

References and Notes

(1) Chakrabartty, A.; Baldwin, R. L. *Adv. Prot. Chem.* **1995**, *46*, 141.
(2) Padmanabhan, S.; Marqusee, S.; Ridgeway, T.; Laue, T. M.; Baldwin, R. L. *Nature* **1990**, *344*, 268.
(3) O'Neil, K. T.; DeGrado, W. F. *Science* **1990**, *250*, 646.
(4) Lyu, P. C.; Liff, M. I.; Marky, L. A.; Kallenbach, N. R. *Science* **1990**, *250*, 669.
(5) Blaber, M.; Zhang, X.-J.; Matthews, B. W. *Science* **1993**, *260*, 1637.
(6) Yang, A.-S.; Honig, B. *J. Mol. Biol.* **1995**, *252*, 351.
(7) DiCapua, F. M.; Swaminathan, S.; Beveridge, D. L. *J. Am. Chem. Soc.* **1991**, *113*, 6145.
(8) Kaltashov, I. A.; Fenselau, C. *Proteins: Struct. Func. Genet.* **1997**, *27*, 165.
(9) Hudgins, R. R.; Mao, Y.; Ratner, M. A.; Jarrold, M. F. *Biophys. J.* **1999**, *76*, 1591.
(10) Hudgins, R. R.; Ratner, M. A.; Jarrold, M. F. *J. Am. Chem. Soc.* **1998**, *120*, 12974.
(11) Hudgins, R. R.; Jarrold, M. F. *J. Am. Chem. Soc.* **1999**, *121*, 3494.
(12) Hol, W. G. J.; van Duijnen, P. T.; Berendsen, H. J. C. *Nature (London)* **1978**, *273*, 443.
(13) Blagdon, D. E.; Goodman, M. *Biopolymers* **1975**, *14*, 241.
(14) Presta, L. G.; Rose, G. D. *Science* **1988**, *240*, 1632.
(15) Forood, B.; Feliciano, E. J.; Nambiar, K. P. *Proc. Natl. Acad. Sci. U.S.A.* **1993**, *90*, 838.
(16) http://www.icpf.cas.cz/jiri/macsimus/default.htm.
(17) Brooks, B. R.; Bruccoleri, R. E.; Olafson, B. D.; States, D. J.; Swaminathan, S.; Karplus, M. *J. Comput. Chem.* **1983**, *4*, 187.
(18) Van Gunsteren, W. F.; Berendsen, H. J. *Mol. Phys.* **1977**, *34*, 1311.
(19) Weiner, S. J.; Kollman, P. A.; Case, D. A.; Singh, U. C.; Ghio, C.; Alagona, G.; Profeta, S.; Weiner, P. *J. Am. Chem. Soc.* **1984**, *106*, 765.
(20) Gorman, G. S.; Speir, J. P.; Turner, C. A.; Amster, I. J. *J. Am. Chem. Soc.* **1992**, *114*, 3986.
(21) Wu, Z.; Feneslau, C. *Tetrahedron* **1993**, *49*, 9197.
(22) Carr, S. R.; Cassady, C. J. *J. Am. Soc. Mass Spectrom.* **1996**, *7*, 1203.
(23) Dugourd, P.; Hudgins, R. R.; Clemmer, D. E.; Jarrold, M. F. *Rev. Sci. Instrum.* **1997**, *68*, 1122.
(24) Hudgins, R. R.; Woenckhaus, J.; Jarrold, M. F. *Int. J. Mass. Spectrom. Ion. Proc.* **1997**, *165/166*, 497−507.
(25) Mason, E. A.; McDaniel, E. W. *Transport Properties of Ions in Gases*; Wiley: New York, 1988.
(26) Hagen, D. F. *Anal. Chem.* **1979**, *51*, 870. Karpas, Z.; Cohen, M. J.; Stimac, R. M.; Wernlund, R. F. *Int. J. Mass Spectrom. Ion Processes* **1986**, *83*, 163. Von Helden, G.; Hsu, M. T.; Kemper, P. R.; Bowers, M. T. *J. Chem. Phys.* **1991**, *95*, 3835.
(27) Counterman, A. E.; Valentine, S. J.; Srebalus, C. A.; Henderson, S. C.; Hoagland, C. S.; Clemmer, D. E. *J. Am. Soc. Mass Spectrom.* **1998**, *9*, 743.
(28) Mesleh, M. F.; Hunter, J. M.; Shvartsburg, A. A.; Schatz, G. C.; Jarrold, M. F. *J. Phys. Chem.* **1996**, *100*, 16082.
(29) Shvartsburg, A. A.; Schatz, G. C.; Jarrold, M. F. *J. Chem. Phys.* **1998**, *108*, 2416.
(30) Okamoto, Y.; Hansmann, U. H. E. *J. Phys. Chem.* **1995**, *99*, 11276.
(31) Go, M.; Go, N.; Scheraga, H. A. *J. Chem. Phys.* **1970**, *52*, 2060.
(32) Creamer, T. P.; Rose, G. D. *Proc. Natl. Acad. Sci. U.S.A.* **1992**, *89*, 5937.
(33) Aurora, R.; Creamer, T. P.; Srinivasan, R.; Rose, G. D. *J. Biol. Chem.* **1997**, *272*, 1413.
(34) Doruker, P.; Bahar, I. *Biophys. J.* **1997**, *72*, 2445.
(35) Arteca, G. A. *Biopolymers* **1995**, *35*, 393.
(36) Sung, S.-S. *Biophys. J.* **1994**, *66*, 1796.
(37) Bertsch, R. A.; Vaidehi, N.; Chan, S. I.; Goddard, W. A. *Proteins* **1998**, *33*, 343.